Available online at www.CivileJournal.org

Civil Engineering Journal

Vol. 5, No. 9, September, 2019

Solving Elasto-Static Bounded Problems with a Novel Arbitrary-Shaped Element

H. R. Khalaj-Hedayati [a], M. I. Khodakarami [a*]

[a] *Faculty of Civil Engineering, Semnan University, P.O.Box 35131-19111, Semnan, Iran.*

Received 23 April 2019; Accepted 26 July 2019

Abstract

A simple method to analysis any arbitrary domain shapes with a single element which based on Decoupled Scaled Boundary Finite Element Method is presented in this paper. The introduced element is based on boundary finite element method which helps to modelling curve and sharp boundaries with acceptable accuracy. Shape functions and mapping functions are similar to Decoupled Scaled Boundary Finite Element Method but locating center origin (LCO) is relocated in this method from corners with direct view to whole domain into shape center and formulation and behavior of the method is developed for the element. The most important advantageous of this technique is ability of solving displacement in domain by solving differential equations which causes more accurate answers in domain. We also perform well-established numerical tests and show the performance of the new element. Results shown us the accuracy and reliable answers for the introduced element. Also some benchmark examples are solved by this method and answers are compared with correct answers and plotted. High accuracy of answers with low cost of calculations and ability of the method to analysis the curve and sharp boundaries are the most important advantageous of this new element.

Keywords: Decoupled Scaled Boundary Finite Element (DSBFEM); Arbitrary-shaped Element; 2D Analysis; Finite Element Method (FEM); Elastostatic; Bounded Domain.

1. Introduction

It is well known that 2D problems can be applied in engineering as well and the results can be reliable for engineering decision. Various types of numerical methods such as Finite Element Method (FEM), Boundary Element Method (BEM), Scaled Boundary Methods (SBFEM), and mesh-less methods are commonly used in order to solve elasto-static and elasto-dynamic problems in two-dimensional problems [1-3] and simulating cracks and fractures in domains [4-5]. All these methods have their own advantageous and disadvantageous. Many types of elements are used in FEM approach in order to solve general or conditional problems, Serendipity and Lagrange elements which belongs to classical FEM [6] and combined elements which developed to solve conditional problems such as, Arnold-Winther stress element, Crouziex-Raviart element, Pi element, Brezzi-Douglas-Marini element, Brezzi-Douglas-Fortin element, Virtual and polygonal elements which have their own conditions to be used [7-12].

One of the desirable methods for solving elastic problems is Boundary Element Method (BEM), in which requires reduced surface discretization and so fewer unknowns are needed to be stored. Moreover, BEM requires a fundamental solution for the governing differential equation in the domain in order to obtain boundary integral equation. In this condition, the coefficient matrices of BEM are much smaller than those of FEM, usually non positive, non-symmetric, and fully populated [13].

* Corresponding author: khodakarami@semnan.ac.ir

http://dx.doi.org/10.28991/cej-2019-03091384

Combining the advantages of FEM and BEM, SBFEM was successfully developed. Using surface finite element, SBFEM discretize only the boundary of the domain by transforming governing partial differential equations to ordinary differential equations, which may solve analytically. SBFEM, which requires no fundamental solution, have also been employed for analysis of elasto-static and elasto-dynamic problem. The method relies on the definition of a scaling center from which the entire boundary is visible. The salient feature of the method is that the discretization is restricted to the surfaces of the polyhedron, thus reducing the dimensionality of the problem by one. Hence, an explicit form of the shape functions inside the polyhedron is not required [14]. Bounded near fields are also modelled by this method and even unbounded domains are modelled by SBFEM in 2D and 3D domains. While the SBFEM has proven its effectiveness in the treatment of 2D boundary value problems with stress singularities, it suffers from reduced convergence rates and accuracy in 3D cases with line singularities. This is due to the then unpreventable occurrence of singularities in the discretized boundary coordinates of the SBFEM [15-16].

During last decades' researchers have also paid attention to mesh-less methods. These methods usually do not require specific meshes, while boundary nodes are needed. Some example of this method are Petrov-Galerkin method [17], Boundary Element free method [18], Local point interpolating method [19], Local boundary integral equation method [20], collocation method [21], Hybrid method [22] and other methods have been employed for numerical solution problems with arbitrary and high wavenumbers [23], numerical solutions of 2D Helmholtz problems with mixed boundary conditions of Dirichlet and Neumann types [24-25].

A modification of SBFEM with diagonal coefficient matrices (DSBFEM) has been proposed by author for solving potential problems and it is applied to solve elastostatic and elastodynamic problems where the Lagrange polynomials is used as mapping functions and also Gauss-Lobatto_Legendre quadrature is employed in order to calculate coefficient matrices [26]. By the way with implementing this technique, the governing equation for each node are independent of the other nodes. And this will reduce the computational costs [27-30].

In this research, the Locating Coordinate Origin (LCO) is relocated to center of area of the problem which causes ability of use any arbitrary shapes of domain as a single element or dividing the domain of problem to any arbitrary shapes to solve (Figure 1). In this paper we use Decoupled Scaled Boundary Finite Element Method in order to solve whole domain by finite element rules. In this way first we divide the boundaries into some nodes (Gaussian nodes) and then we locate the Locating Coordinate Origin (LCO) at the center of area of the domain shape. This technique will help us to solve any arbitrary domain shapes.

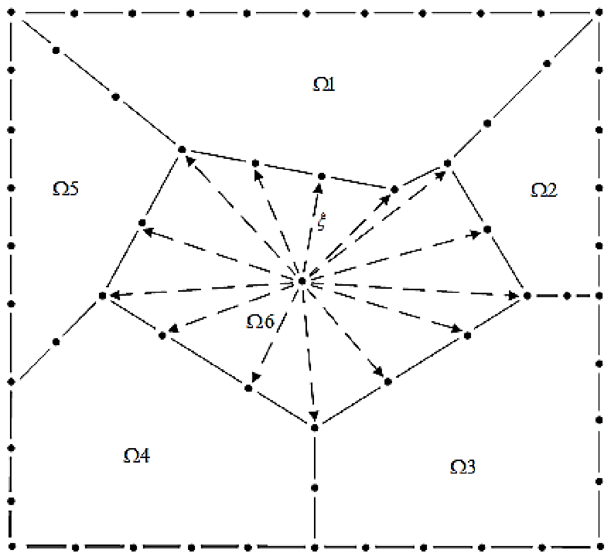

Figure 1. Ability of suggested method to calculate any arbitrary domain shape or dividing domain to any arbitrary sub-elements shapes

The motivation of this research comes from the fact of development of mesh-less methods is still a great challenge for researchers to accurate and optimize the answers in other hand the domain shape difficulties can lead us to make many mistakes and deliberately ignore of some aspects of answers in complex domains. By advantageous of DSBFEM curved and direct boundaries can be modeled and solved with high accuracy and no approximation or missing domain is needed. The suggesting technique calculate the stiffness matrices by innovative way based on DSBFEM method and force vector by DSBFEM method. Achieved Matrices and vectors will use in Finite Element fundamental equation to calculate displacement of each boundary nodes and strain interpolation, domain stresses and displacements will calculate by DSBFEM again.

In this method as mentioned above, Stiffness Matrix and Force vectors are calculated by DSBFEM and then fundamental FEM equation is solved by the achieved matrix and vector, the results is boundaries displacements for element.

The method is applied to solve some benchmark examples and the results are shown. The results shown high accuracy and reliable answers for the suggested method.

2. DSBFEM Formulation of Continuum Mechanics Based 2D Elements

The continuum mechanics displacement based bar finite element have been proposed. While bar elements are usually using to solve truss elements, it can also use as a main concept of the presented method. Here we present the concepts of suggested method for explaining the new developments in this research. The basic rules and concepts of DSBFEM is presented in previous author's papers. In this method, the domain will consider as an element and locating coordinates origin (LCO) is chosen at center of the area of element which can cause to calculate huge elements with arbitrary shapes. The global Cartesian coordinates in 2D problems are (x, y) which by using Lagrange polynomials would be transmitted to local coordinate(ξ, η) , where ξ is radial coordinates which varies from 0 at LCO to 1 at boundary nodes and η is tangential coordinates which varies between -1 and 1 on the boundaries(Figure 2).

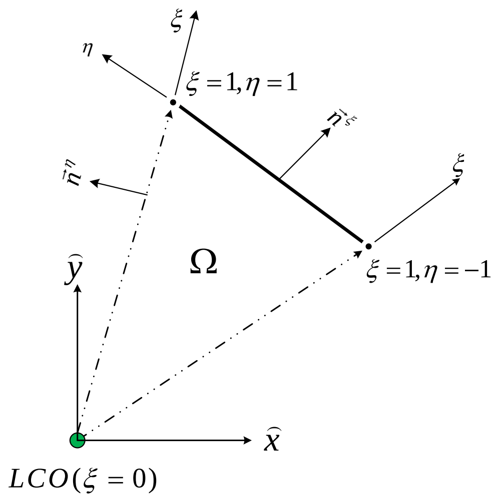

Figure 2. Modeling 2D bounded domain in the scaled boundary system with local coordinate origin (LCO) and related local axes

Each node at the boundaries can be transmitted to local coordinates by these mapping functions by Equation 1:

$$\{x(\eta)\} = [\phi(\eta)]\{x\} \tag{1}$$

Where,$\{x\} = [x \;\; y]^T$ denotes the global coordinates of boundary nodes, $\phi[(\eta)]$ is a $2n_\eta + 1$ matrix and $n_\eta + 1$ is number of nodes in the element. For a $n_\eta + 1$ node element, a Lagrange polynomial of n_η is used, these polynomials for ith point will be calculated by Equation 2:

$$\phi_i(\eta) = \prod_{k=1, k\neq i}^{n_\eta+1} \frac{\eta - \eta_k}{\eta_i - \eta_k} \tag{2}$$

Considering Equation 2, the Lagrange polynomials have the properties of the Kronecker delta at any control point$\left(\varphi_i(\eta_j) = \delta_{ij}\right)$. As it is clear, to prepare n_η parent element, $(n_\eta + 1)$ nodes are required, where two end-nodes are located at the extremity $\eta = \pm 1$ of the element and other remained nodes are located at Gauss-Lobbato-Legendre points. These points are the first roots of the first order derivative of order n_η Legendre polynomials Equation 3:

$$\frac{d}{d\eta} P_{n_\eta}(\eta) = 0 \tag{3}$$

Where, the Legendre polynomials of order n_η is expressed using Rodrigues' formula as Equation 4:

$$P_{n_\eta} = \frac{1}{2^n n!} \cdot \frac{d^{n_\eta}}{d\eta^{n_\eta}} \left[\left(\eta^2 - 1\right)^{n_\eta} \right] \tag{4}$$

Lagrange polynomials is used to interpolate the geometry of the problem. In the DSBFEM, special polynomials $N(\eta)$ are used as shape functions, in order to interpolating the displacement of each node at the boundaries and whole domain and the derivatives of displacement across the element. These polynomials have two specific characteristics, the shape function have property of Kronecker Delta, and their first derivatives are equal to zero at control points. The shape function is expressed in Equation 5:

$$N_i(\eta) = \sum_{m=1}^{2n_\eta+1} a_m \eta^m \tag{5}$$

The solution procedure for any engineering problems using these proposed elements has two steps:

- Solution in each element
- Solution for whole domain of the problem

All formulation of DSBFEM is available and reliable in the element; so the governing equation for engineering problems is solved by the rules of DSBFEM for 2D problems as Equation 6:

$$\xi.D_{ii}^0.u_{i,\xi\xi}(\xi)+D_{ii}^1.u_{i,\xi}(\xi)=-\xi.F_i^b(\xi) \tag{6}$$

Using basic rules of DSBFEM lead us to calculate $[D^0]$ and $[D^1]$ by Equations 7 and 8:

$$\left[D_{ij}^0\right]=\delta_{ij}w_i\left[B^1(\eta_i)\right]^T[D]\left[B^1(\eta_i)\right]\left|J(\eta_i)\right|d\eta \tag{7}$$

$$\left[D_{ij}^1\right]=\delta_{ij}w_i\left[B^1(\eta_i)\right]_{,\eta}^T[D]\left[B^2(\eta_i)\right]\left|J(\eta_i)\right|d\eta \tag{8}$$

Where $[B^1]=[b^1(\eta)][N(\eta)]$ and $[B^1]=[b^1(\eta)][N(\eta)]_{,\eta}$. These $[b^1]$ and $[b^2]$ matrices are calculating by Equations 9 and 10:

$$\left[b^1(\eta)\right]=\frac{1}{|j(\eta)|}\begin{bmatrix} y(\eta)_{,\eta} & 0 \\ 0 & -x(\eta)_{,\eta} \\ -x(\eta)_{,\eta} & y(\eta)_{,\eta} \end{bmatrix} \tag{9}$$

$$\left[b^2(\eta)\right]=\frac{1}{|j(\eta)|}\begin{bmatrix} -y(\eta) & 0 \\ 0 & x(\eta) \\ x(\eta) & -y(\eta) \end{bmatrix} \tag{10}$$

Where $J(\eta)$ indicates the Jacobian matrix and can be written in Equation 11:

$$J(\eta)=\begin{bmatrix} x(\eta) & y(\eta) \\ \dfrac{\partial x(\eta)}{\partial \eta} & \dfrac{\partial y(\eta)}{\partial \eta} \end{bmatrix} \tag{11}$$

The differential element of area in the global coordinates $dxdy$ is evaluated by Jacobian matrix of the transformation in the local coordinates Equation 12:

$$dxdy=\xi\left|J(\eta)\right|d\xi d\eta \tag{12}$$

The characteristic of D^0 and D^1 causes that according to boundaries form some or whole matrix elements be zero. It is clearly shown in (Figure 3). This type of matrices happens while D^0 is related to first derivative of nodes coordinate and D^1 is related to second derivative of nodes coordinates. So in direct boundaries the second derivative of term D^0 will be zero and it will take value when the boundaries were not direct.

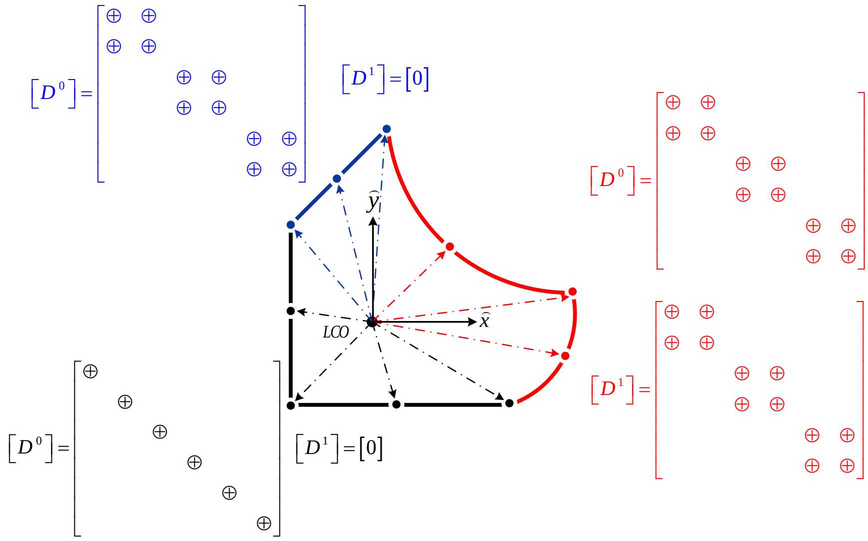

Figure 3. The effects of boundaries configuration on the coefficient matrices (D0 and D1) in the Decoupled Scaled Boundary Method (DSBFEM)

To solve and calculate the vectors and matrices in Equations 7 and 8, the Gauss-Lobatto-Legendre numerical integration method is applied in numerical integration method calculate the values of the coefficient matrix in GLL according to the node element that corresponds to the points and also features a shape function used, resulting diagonal matrix of coefficients used in the equation. Weight coefficients used in the method of integration is calculated using Equation 13:

$$w_i = \frac{w}{n_\eta(n_\eta+1)(P_{n_\eta}(\eta_i))} \rightarrow i = 0,1,2,\cdots,(n_\eta+1) \tag{13}$$

Where, δ_{ij} denotes the Kronecker Delta which results in diagonal matrices. So, the system of partial differential Equation 6 may be expressed as a single differential equation regarding to specified point *i*.

2.1. Strain Interpolating Technique for Suggested Element

Two methods of interpolating the strains for introduced element are used. First to interpolate the boundaries and second for calculating in domain. As mentioned before, this element is made of DSBFEM and general formulation of that technique is acceptable in this method, so boundaries strains can be calculated by the methods of that technique and domain strains can be calculated by solving differential equations.

2.1.1. Calculating Boundaries Strains

To calculate boundaries displacements, special shape function is used which mentioned before and will define completely here. These functions have property of Kronecker Delta function and their firs derivatives are equal to zero at any given control point Equations 14 and 15.

$$N_\alpha(\eta_\beta) = \delta_{\alpha\beta} \tag{14}$$

$$N_{\alpha,\eta}(\eta_\beta) = 0 \tag{15}$$

For an $(n_\eta + 1)$ node element, these shape functions are expressed as a polynomial of degree $2n_\eta - 1$ that has $2n_\eta$ unknown constant coefficients as Equation 16:

$$N_i(\eta) = a_0 + a_1\eta + a_2\eta^2 + a_3\eta^3 + \ldots + a_{2n_\eta-1}\eta^{2n\eta-1} \tag{16}$$

The constant coefficients of the polynomial are obtained using Equations 14 and 15. The shape function of three nodes element is shown in (Figure 4) and tables of constant coefficients is shown in [28].

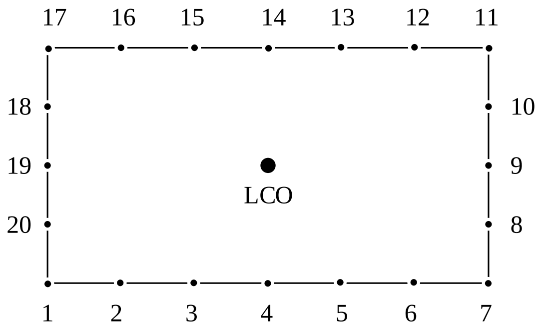

(a)

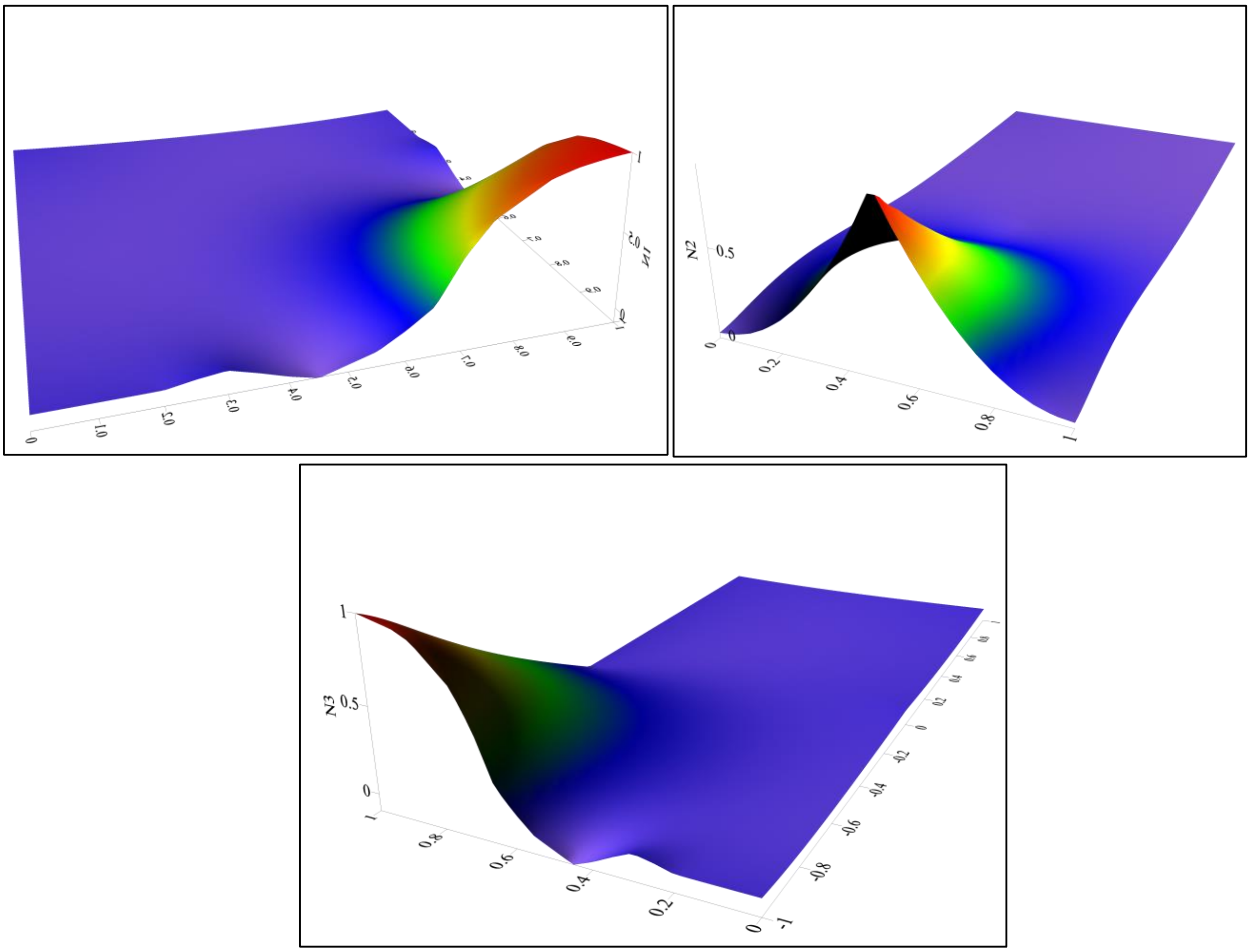

(b)

Figure 4. Schematic of 20-node proposed element based on DSBFEM: (a) geometry of the element, (b) shape functions for three first-node (N1, N2 and N3) of this element

2.1.2. Calculating Domain Strains

In order to calculate domain strains we have to find fundamental equation of displacement in domain which is developed in following scopes and it is innovative for the suggested technique.

2.1.3. Calculating Stress in Domain

Also the stresses among the ξ direction can be calculated with Equation 17. This Equation is completely comes from DSBFEM and it is reliable in presented method Equation 17.

$$[\sigma]=[D]\left(\left[B^1\right]\{u\}_{,\xi}+\frac{1}{\xi}\left[B^2\right]\{u\}\right) \tag{17}$$

Where among the general direction which if the boundaries were direct, the second term in parentheses will be zero and the stresses will calculate by only the first term.

3. Finite Element Procedure

By calculating each sub-element local stiffness matrix and assembling global matrix of stiffness the whole domain stiffness matrix will be achieved and fundamental equation of FE can be solved in order to calculate displacement vectors Equation 18.

$$[K]\{u\}=\{F\} \tag{18}$$

Where K is $2n \times 2n$ matrix which n is the nodes amount, U and F are $2n \times 1$ vectors.

3.1. Stiffness Matrix Creation

To create the stiffness matrix for an element, we consider that each node at boundaries is connected to the LCO by a line which has the properties of the whole domain. This lines are connected together at LCO. All this lines have their own stiffness in their local coordinates let us call these lines sub-elements. Each line of stiffness matrix is made of applying a unit displacement at any degree of freedom and calculate the reaction of other degrees of freedom. This procedure needs to be calculated in two main steps:

- First: Fixing all degrees of freedom except one we want to apply a unit displacement and Calculate the respectively force which made by the unit displacement at intersection point of the sub-elements (LCO).
- Second: Divide the calculated force at LCO between all the sub-elements respecting to their stiffness.

3.1.1. Fixing all Degrees of Freedom except One We Want to Apply Unit Displacement

Let us consider the whole domain consist of some sub-elements which connecting boundary nodes to LCO. These sub-elements in their nature can be assumed as a bar element and since we are calculating at 2D space, each node has two degrees of freedom while we regardless the flexural freedoms. These sub-elements are connecting together at LCO, so we can consider LCO as a restrain for each sub-element. It is clear that this restrain is not rigid and also one can find out that the rigidity of this restrain is consist of rigidity of all incoming sub-elements (Figure 5).

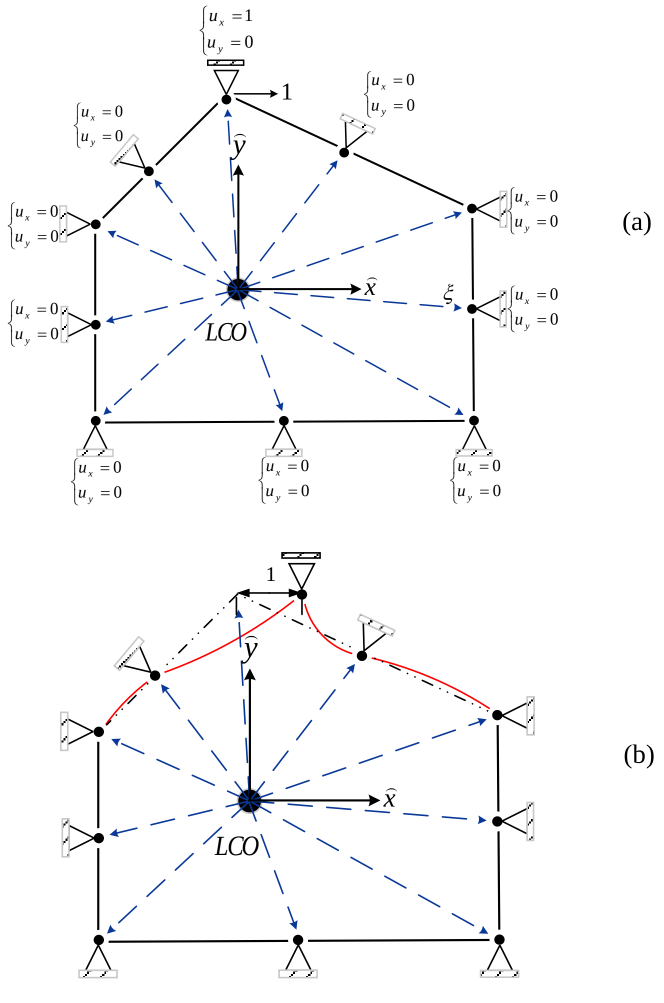

Figure 5. A DSBFEM-sub-element in local coordinates system: (a) 10-node arbitrary-shaped element and its discretization, (b) deformed shape subjected to unique displacement at the released degree of freedom

The produced force due to displacement of a node at local coordinate can be calculated with Equation 19:

$$\{F\} = \xi\left[D^0{}_i\right]\{u'\} \tag{19}$$

By knowing that when each degree of freedom is released to move freely in case of non-exist of external forces, the governing differential equation for element is linear in corresponding to ξ by solving Equation 6 where expressed in Equation 20:

$$\{u\}_i(\xi) = \{A\}_i\xi + \{B\}_i \tag{20}$$

Where in Equation (20) the 'B_i' term is displacement at LCO which is zero in this case and due to boundary conditions at $= 1$, and 'A_i' term Equation 19 can be 1 corresponding to applied displacement at node.

As shown in Equation 20, if we consider 'k' for calling released degree of freedom, in situation of applying unique displacement at node k, we can simply find out Equation 21:

$$u_i(\xi) = \begin{cases} 0, i \neq k \\ \xi, i = k \end{cases} \qquad u_i'(\xi) = \begin{cases} 0, i \neq k \\ 1, i = k \end{cases} \tag{21}$$

As we consider all boundaries to be direct according to (Figure 5) we have just $[D^0]$ term in our equations. By considering the LCO as a restrain its rigidity is made of all arrival sub-elements to the LCO, this rigidity can be calculating by Equation 22:

$$\left[D^0\right]_{LCO} = \sum_{i=1}^{n}\left[D^0\right]_i \tag{22}$$

Where n is the amount of nodes which considered at the boundaries. The forces which calculated by Equation 19 can make u' at LCO. As it is clear that this u' can't be different in a same point, so this term can calculate by Equation 23:

$$\{u'_{LCO}\}_i = \xi\left[D^0\right]_{LCO}^{-1}\left[D^0\right]_i\{u'_i\} \tag{23}$$

3.1.2. Divide the Calculated Force at LCO between All Sub Elements

The produced force at LCO due to applying a unit displacement at a degree of freedom, can be divide between all sub-elements which arrived at LCO. There are two situations can be considered.

- The produced force at LCO is turning back to the released degree of freedom
- The produced force at LCO is dividing to another degrees of freedom

General formula to calculate refracting force to each sub-element can be written as Equation (24).

$$\left[D^0\right]_i\{u''(\xi)\}_i - \{F(\xi)\}_i = 0 \tag{24}$$

By using Equation 19 in Equation 24, the term $\{F(\xi)\}_i$ can be calculated as Equation 25 for k-element:

$$\{F(\xi)\}_i = \xi[D]^0{}_i(u'_{LCO_i} + \xi(u'_k - u'_{LCO_i})) \tag{25}$$

Solving Equation 25 leads us to calculate displacement in whole domain among ξ direction as Equation 26:

$$\{u(\xi)\}_i = \frac{1}{6}\xi^3(\{u'\}_i - \{u'_{LCO}\}) + \frac{1}{2}\xi^2\{u'_{LCO}\} + \{u'_{LCO}\}\xi + \{u'_{LCO}\} \tag{26}$$

By solving Equation 25 and Equation 26 the forces which created by unique displacement at a degree of freedom can be calculated at the other nodes and this technique can help us to assemble the stiffness matrix of whole domain.

The general equation $[K]\{u\} = \{F\}$ can be obtained to calculate the nodes displacement in case of static loads. The first derivate of displacement (u') can be calculated by equilibrium of internal and external forces at each node.

After calculating the displacement and first derivative of displacement at each node, the most important factor is to calculate these amounts at LCO which can leads us to extract the governing equation in whole domain of the problem, in this way we use we use the force equilibrium rule at LCO. This equilibrium at LCO can help us to calculate the displacement at LCO.

By this technique we can calculate the displacement at each node and then the strain and stresses at whole domain is available.

And the stiffness matrix can be created by Equation 27 for any sub-element which called *i* due to release of *k* sub-element and *j* is a counter which varies between 1 and n:

$$\{k_i\}_k = \begin{Bmatrix} k_{i(2j-1)} \\ k_{i(2j)} \end{Bmatrix} = \left[D^0\right]_k . \left\{u_k'^{*}(\xi=1)\right\}_i \tag{27}$$

Where $u_k'^{*}$ is defined in Equation 28:

$$\left\{u'^{*}(\xi)\right\}_k = \frac{1}{2}\xi^2(\{u'\}_k - \{u'_{LCO}\}_i) + \xi.\{u'_{LCO}\}_i + \{u'_{LCO}\}_i \tag{28}$$

It is clear that the stiffness matrix is symmetric and definitely positive.

To calculate each sub-element displacement among the ξ direction according to Equation 23 term $\{u'\}_i$ can be calculated by (Equation 21) as Equation 29:

$$\{u'\}_i = \{u'(\xi=1)\}_i = \left[D^0\right]^{-1}_i . \{F(\xi=1)\}_i \tag{29}$$

As mentioned above, the term u'_{LCO} can be calculated by Equation 23 as Equation 30:

$$\{u'_{LCO}\} = \frac{3}{4}\left[\{u\}_i - \{u_{LCO}\} - \frac{1}{6}\{u'\}_i\right] \tag{30}$$

By using equilibrium at LCO, the term u_{LCO} can be calculated by Equation 31:

$$\{u_{LCO}\} = \left[D^0\right]^{-1}_{LCO}\left[\sum_{j=1}^{N}\left[D^0\right]_j\left(\{u\}_j + \frac{1}{6}\{u'\}_j\right)\right] \tag{31}$$

3.2. Force Vector Creation

As mentioned above, this technique is made of DSBFEM for calculating stiffness matrix and force vectors, so for calculating force vectors formulation of DSBFEM is reliable Equation 32.

$$\{F^b(\xi)\} = \int_{-1}^{+1}[N(\eta)]^T\{f^b(\xi,\eta)\}\left|J(\eta)\right| \tag{32}$$

4. Summary of Presented Method

According to presented formulations as it is depicted in Figure 6, the summary of method can be shown by an algorithm as follow:

- Discretizing problem into any arbitrary shapes and boundary nodes;
- Transferring coordinates to ξ,η system by Equation 1;
- Calculating $[b^1(\eta)], [b^2(\eta)]$ by Equation 9 and Equation 10;
- Creating $[D^0], [D^1]$ matrices by Equation 7 and Equation 8;
- Calculating $\{u'_{LCO}\}$ due to boundary nodes release by Equation 23;
- Assembling stiffness matrix by Equation 27 and Equation 28;
- Calculating boundary nodes displacement by FEM formulation $[K]\{u\} = \{F\}$;
- Calculating boundary nodes $\{u'\}$ by using summation of internal and external forces at boundary nodes and using Equation 19;
- Calculating displacement formulation among ξ direction by using Equation 26;
- Calculating displacement at LCO by Equation 31;
- Using displacement at LCO in Equation 30 to calculate $\{u'\}_{LCo}$;
- Calculating stresses among ξ direction by Equation 1.

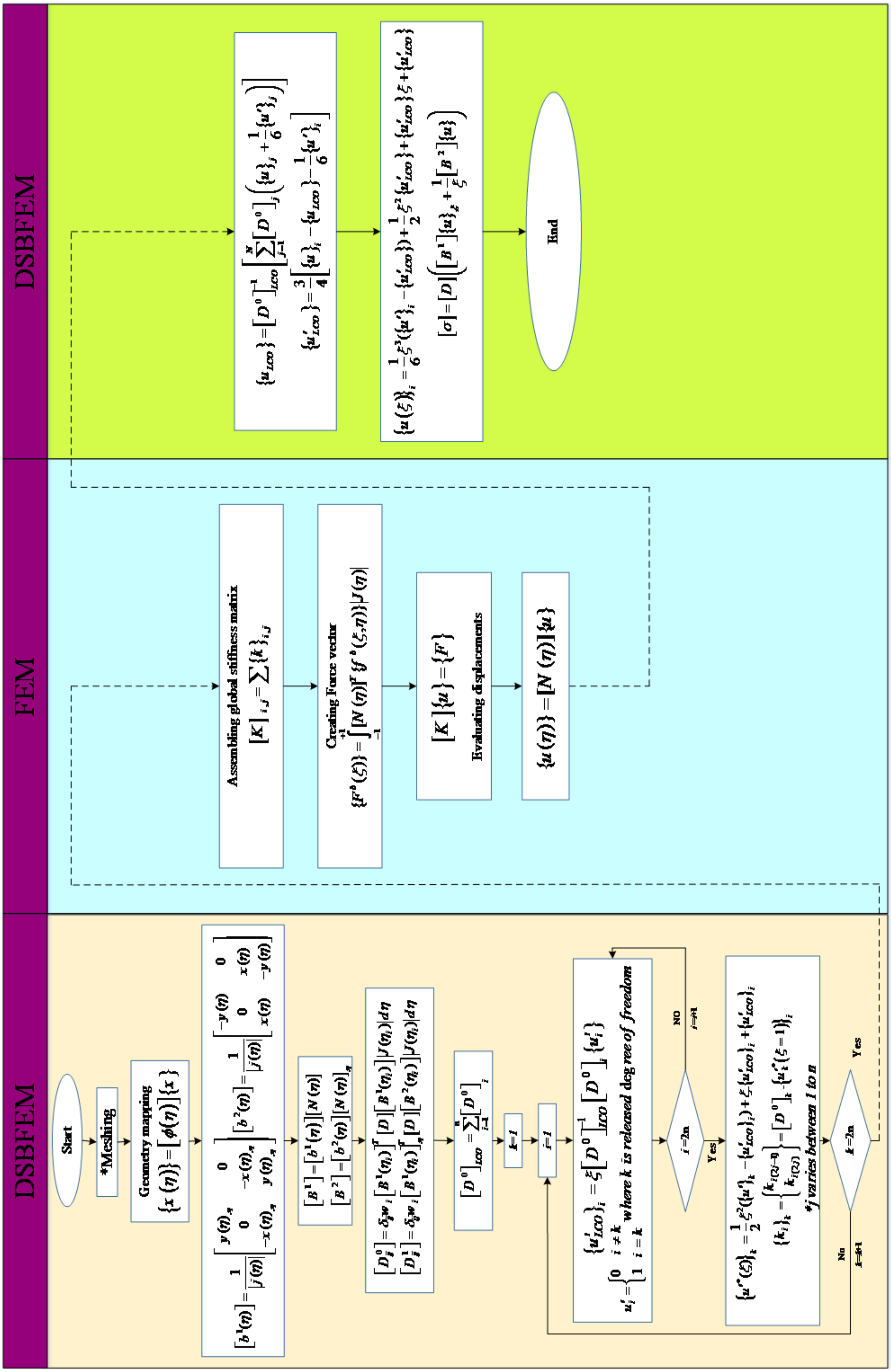

Figure 6. Summary of presented method

5. Numerical Examples

To verify the presented technique, some benchmark examples are solved. The results are monitored and graphs are shown.

5.1. Simple both-end Fix Beam

A simple both-end fix deep beam is obtained due to distributed traction $\sigma_{yy} = -1\frac{kN}{m^2}$. The dimensions are $3m \times 1m$ and thickness $1m$. Poison ratio of material ($\nu = 0.2$) the elasticity module is $2 \times 10^5 \frac{MN}{m^2}$ as shown in (Figure 7). The problem is solved by dividing the whole domain in various amount of elements and sub-elements.

The modelling shows the accuracy of the method while the boundaries divided to a few number of boundary nodes and also the accuracy of answer will improve by adding more boundary nodes to domain discretization. It is illustrated in the results when you increase the calculation costs, although the matrices are diagonal and equations are decoupled which causes low computation cost in comparison with common methods, the high accurate results can be reached.

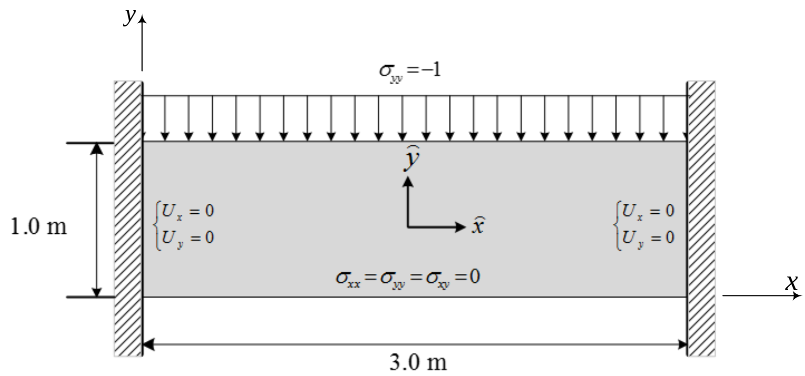

Figure 7. First example: geometry and boundary conditions of the problem in global coordinates system

The whole domain is divided to multi nodes and results is monitored by this deviation, the deviation is shown in Figure 8.

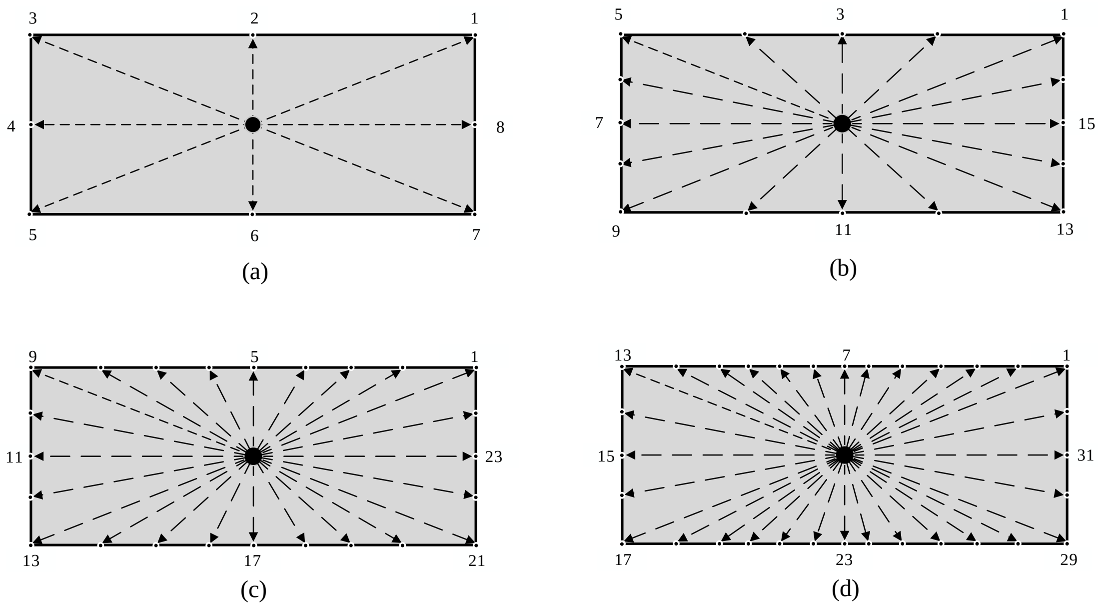

Figure 8. First example: discretizing the geometry of the problem using (a) 8-node element, (b) 16- node element, (c) 24-node element and (d) 32-node element

Mid-line displacement is also compared with reference values and result is plotted in Figure 9.

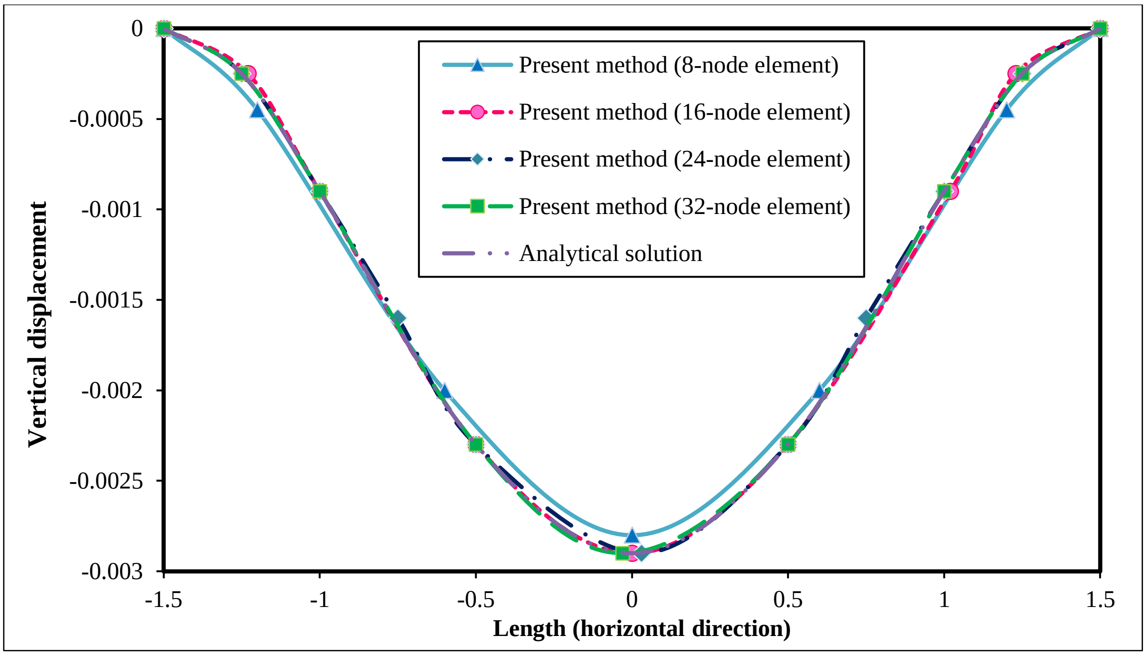

Figure 9. Comparing the results for vertical displacement component between the presented method and analytical solution along $\hat{x}$ axis, $\hat{y} = 0$ (which adopted from [29])

Also effects of increasing boundary nodes on accuracy of answers is plotted and results is shown (Figure 10).

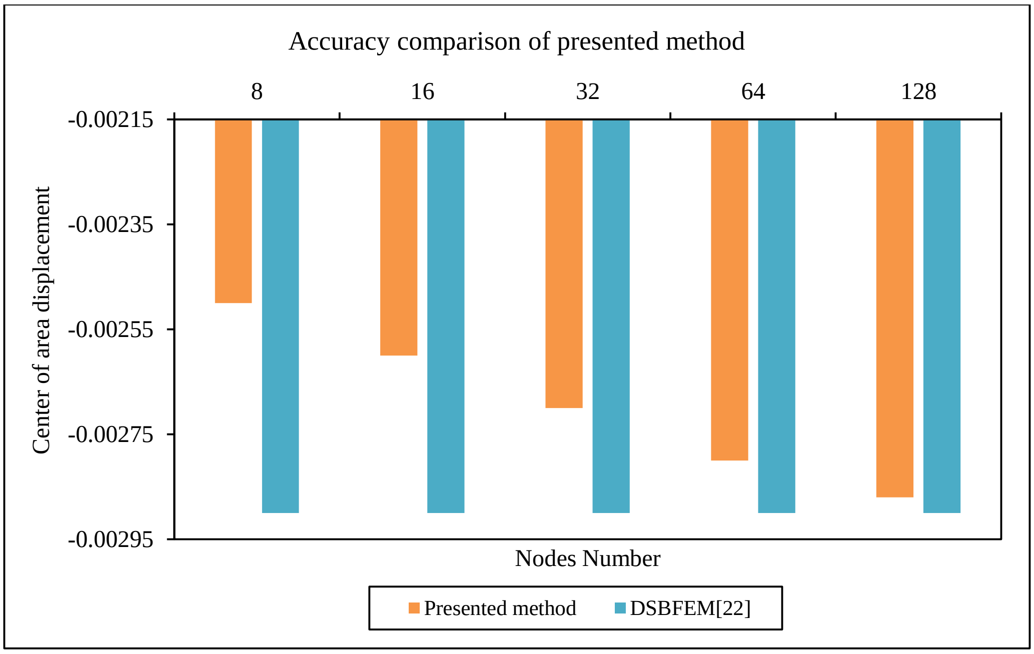

Figure 10. Effects of increasing boundary nodes of suggested element in accuracy of answer (which adopted from [29])

Displacement contour in Y direction is shown in Figure 11.

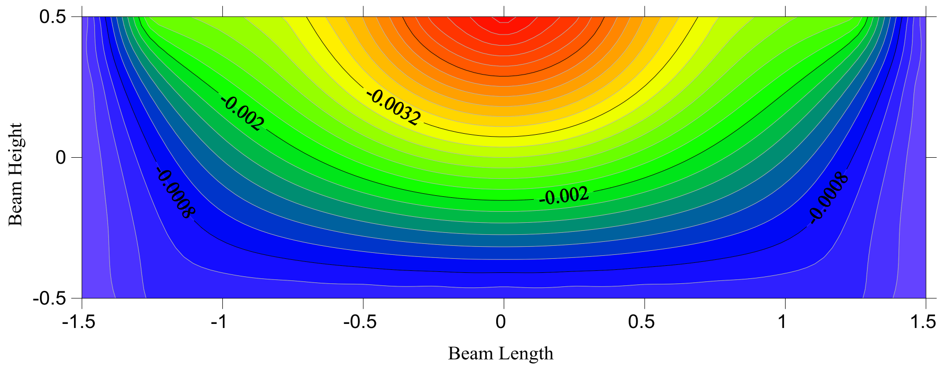

Figure 11. Contour plots of vertical displacement for the first example using a 16-node element in the proposed method

5.2. Pedestal Subjected to Vertical Stress

A pedestal shown in Figure 12 subjected to vertical stress is considered and solved by presented method. The distributed traction $\sigma_{yy} = -1\frac{kN}{m^2}$ is monitored to find out the accuracy of presented method. The dimensions of the beam are $2m \times 2m$ with unit thickness, $= 2000\frac{kN}{m^2}, \nu = 0.2$. The geometry of problem is shown in Figure 13. The problem is solved by an eight-node element (see Figure 14) and results is monitored. The displacement at top surface is monitored and also the domain answers are compared with strength of material solution.

It is shown that the presented method solution for the problem is reliable for engineering decision even by comparing the answers with mechanical exact solution. The answers of this problem are based on an 8 node discretization of domain which are the lowest cost of calculation in presented method with a 16×16 stiffness matrix. It is completely clear that computing a 16×16 matrix is faster than other common methods of stiffness matrix creation and answers are very near to the exact amounts.

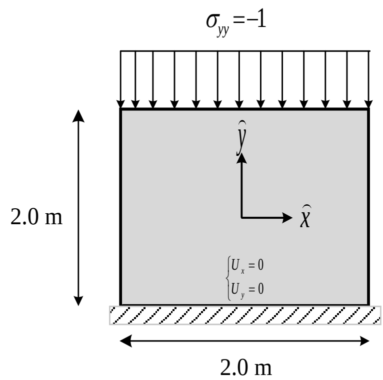

Figure 12. Geometry and boundary conditions of the problem in global coordinates system

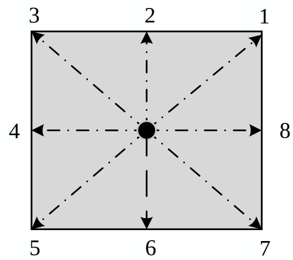

Figure 13. Simulation of the geometry of the problem domain using an 8-node element

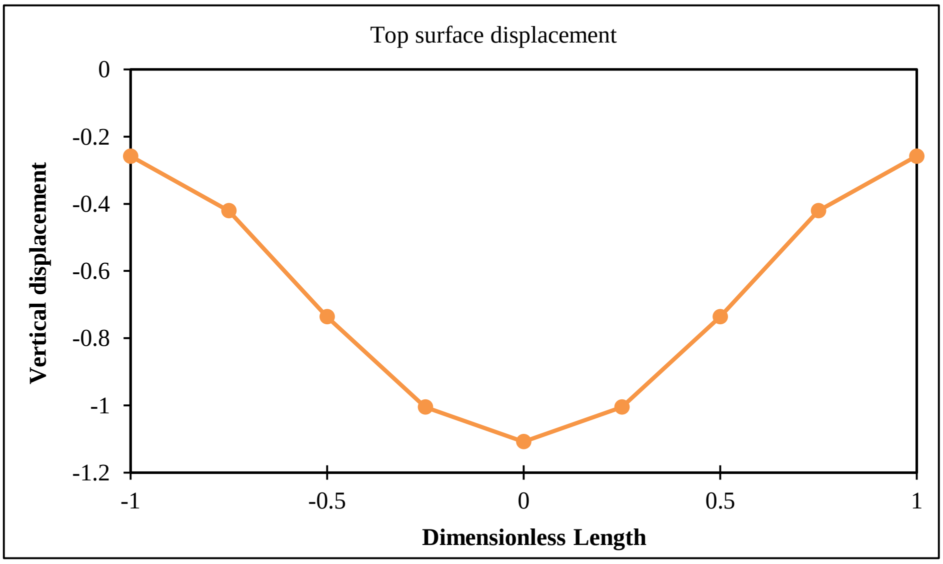

Figure 14. Pedestal top surface displacement

As it is shown in Figure 14 the top boundary displacement is compatible and no breaks can be seen. Also in whole domain is same as shown in Figure 15.

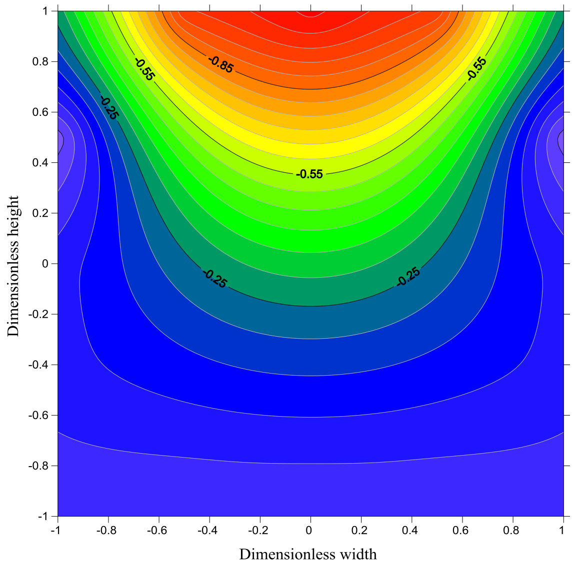

Figure 15. Domain displacement contour Y direction (Labels are dimensionless)

By using mechanical solution, the displacement at top surface is equal to 1. The variation of displacement at mid vertical line is monitored and results is shown in Table 1.

Table 1. Mid vertical line displacement in comparison of presented method and strength of material solution

Height	Displacement (presented method)	Mechanical solution
2	-1.1	-1
1.5	-0.79	-0.75
01	-0.48	-0.5
0.5	-0.24	-0.25
0	0	0

5.3. Cantilever with Concentrated Force

A cantilever beam with a concentrated force at its edge is modelled. The finite element solution of nodes displacements is calculated in Chandrupatla (2002) [31]. The geometry of problem is shown in Figure 16. Module of elasticity is $3 \times 10^7\ kg/m^2$ and $\nu = 0.2$.

The effect of boundary nodes increasing is illustrated in this varied boundary condition problem. The results shown us the increasing accuracy of answers by increasing boundary nodes near the point pf force effect where shown in Figure 17. The boundary nodes discretization in this problem is asymmetric with high density near the force effect point and low number of boundary nodes in far bounds from the force.

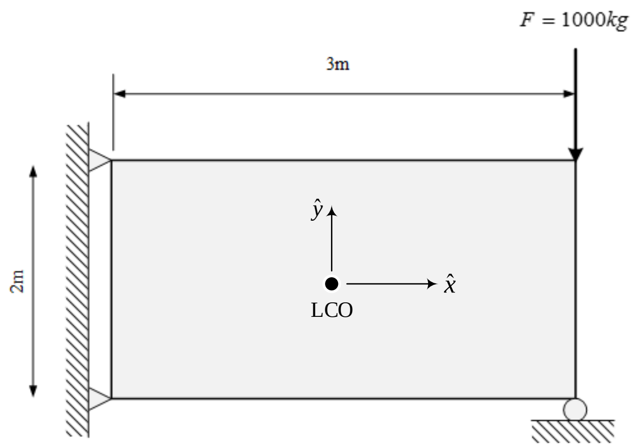

Figure 16. Geometry and boundary conditions of the problem in global coordinates system

The accuracy of presented method can be increased by increasing the number of boundary nodes. The results are shown in Figure 17.

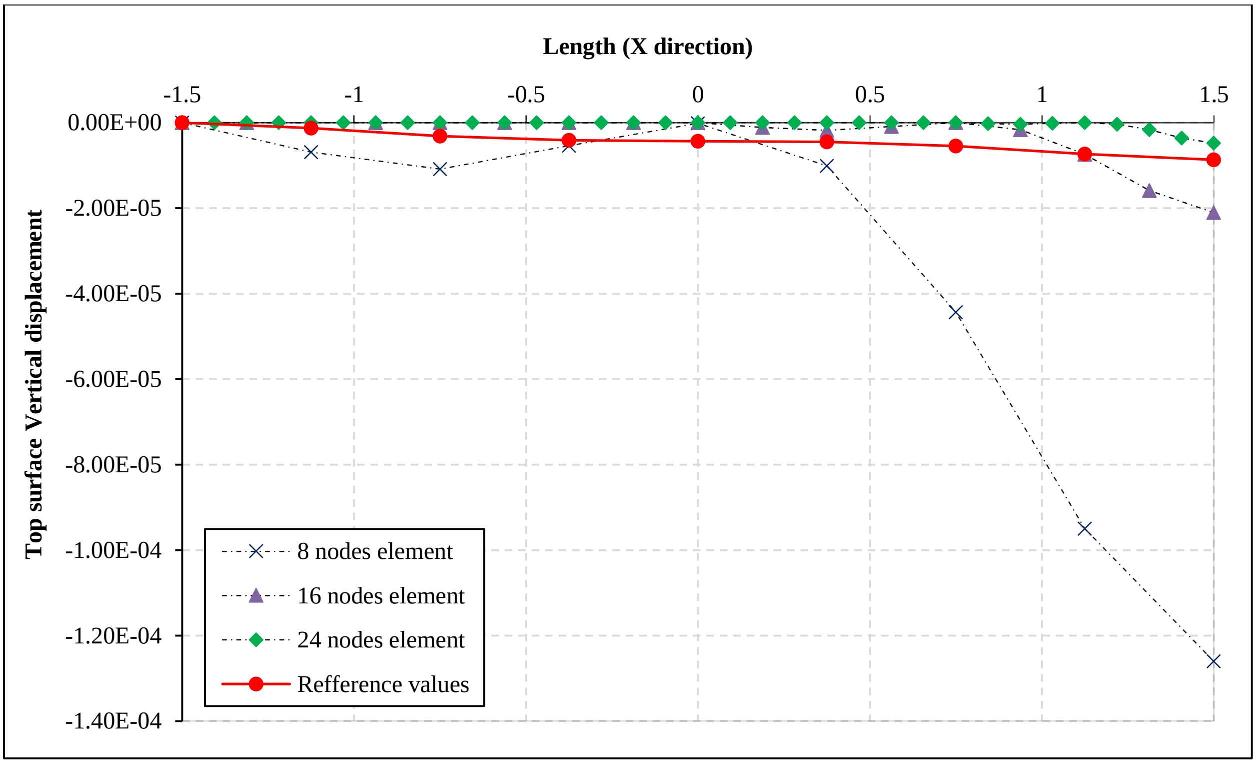

Figure 17. Comparison between the results of vertical displacement component prepared by the presented method and FEM [31] along $\hat{x}$ axis $\hat{y} = 1$

5.4. Rectangular Plate with Side Partially Supported

In this example the rectangular plate presented in Figure 18 is analyzed. Despite the simple geometry and uniform loading condition a more difficult problem is obtained, in which a discontinuous traction singularity can be observed in the middle of the supported side. Since there are no analytical solutions available, a comparison of the results obtained. The displacement of node A due to increasing top surface nodes is plotted and compared with other methods. The accuracy of presented method is monitored and compared with other methods by increasing the nodes number. As illustrated in (Figure 19.).

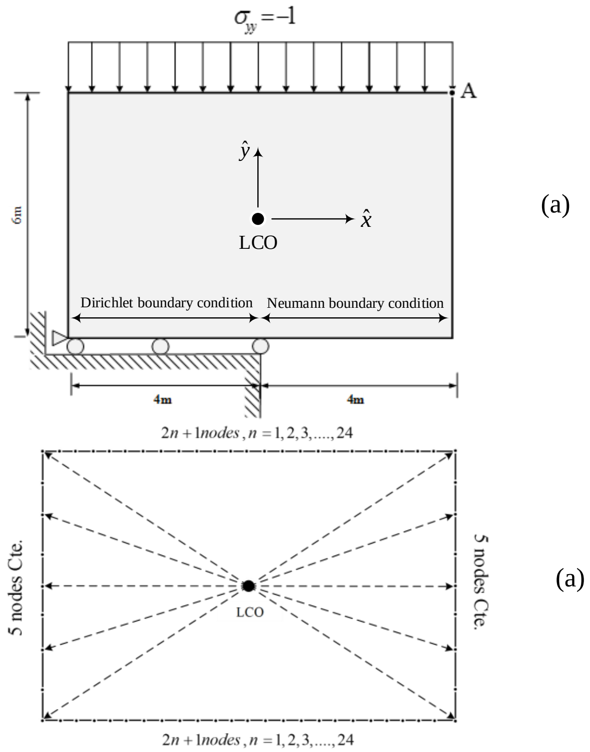

Figure 18. A rectangular plate with uniform loading and discontinuous supporting in bottom surface; (a) geometry and boundary conditions of the problem in global coordinates system and (b) domain discretization using various elements

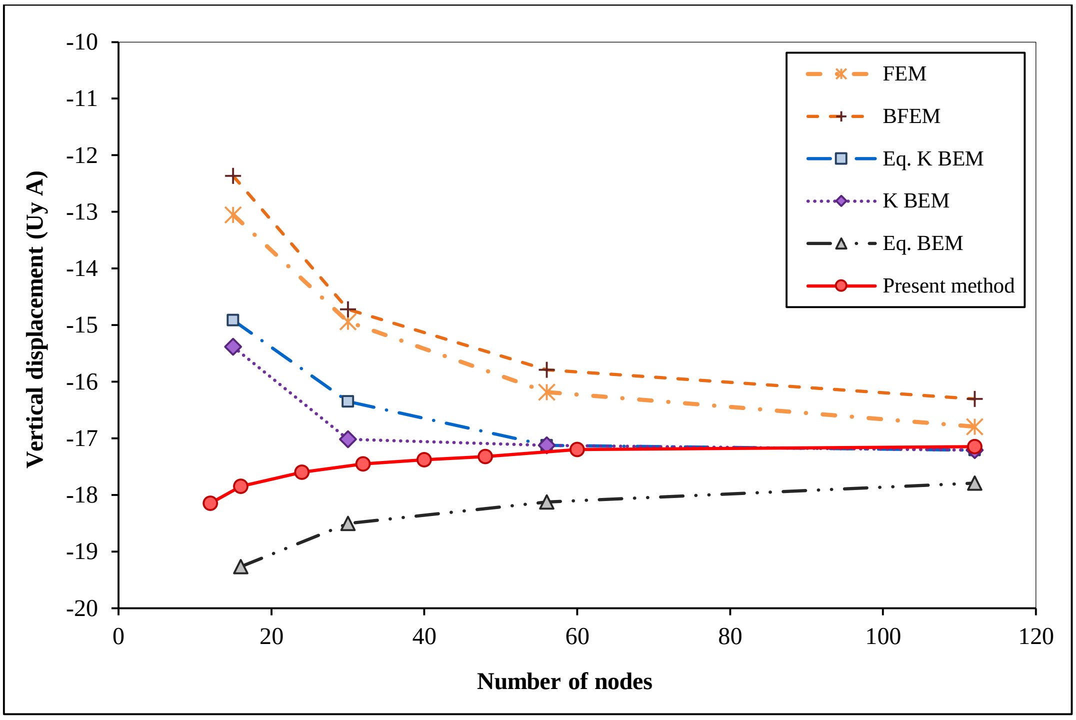

Figure 19. Comparison of the convergence in the results which are prepared by the proposed method of other numerical method (which are adopted from [32])

6. Conclusion

In this research, a modification on the novel element in finite element analysis based on the decoupled scaled boundary finite element method has been studied. The procedure of the modeling and solution of the 2D elastostaic problems are similar to the DSBFEM. The difference in the proposed approach is discretization of boundaries by new higher-order sub-parametric elements and the control points, and also, using Gauss-Lobatto-Legendre quadrature the coefficient of matrices of equation system became diagonal. The most important change in the previous works was relocating LCO to the center of area of the element which leads to a system of decoupled governing equations for entire system. The ability of presented method to model arbitrary shapes as a unique element with no needs to divide it to any sub-elements is its positive point. The accuracy of presented method in comparison with other methods is very attractive. Less calculation nodes, higher speed of calculation, reduced matrices for stiffness and solution procedures, low cost of calculation and in other hand the acceptability of answers in comparison of other techniques is the main aspects of presented method. Presented method can be applied to solve various type of engineering problem with good reliability of answers.

7. Conflicts of Interest

The authors declare no conflict of interest.

8. References

[1] Bathe, Klaus-Jürgen, Finite element procedures. Klaus-Jurgen Bathe, (2017).

[2] Brebbia, C. A., J. Dominguez, and J. L. Tassoulas. “Boundary Elements: An Introductory Course.” Journal of Applied Mechanics 58, no. 3 (1991): 860. doi:10.1115/1.2897280.

[3] Wolf, J.P., and C. Song. “The Scaled Boundary Finite-Element Method - A Primer: Derivations.” Advances in Computational Structural Mechanics (n.d.). doi:10.4203/ccp.55.2.3.

[4] Hell, Sascha, and Wilfried Becker. “An Enriched Scaled Boundary Finite Element Method for 3D Cracks.” Engineering Fracture Mechanics 215 (June 2019): 272–293. doi:10.1016/j.engfracmech.2019.04.032.

[5] Song, Chongmin, Ean Tat Ooi, and Sundararajan Natarajan. “A Review of the Scaled Boundary Finite Element Method for Two-Dimensional Linear Elastic Fracture Mechanics.” Engineering Fracture Mechanics 187 (January 2018): 45–73. doi:10.1016/j.engfracmech.2017.10.016.

[6] Strang, Gilbert, and George J. Fix. An analysis of the finite element method. Vol. 212. Englewood Cliffs, NJ: Prentice-hall, 1973.

[7] Zienkiewicz, O.C., R.L. Taylor, and J.Z. Zhu. "Adaptive Finite Element Refinement." The Finite Element Method Set (2005): 500–524. doi:10.1016/b978-075066431-8.50182-x.

[8] Brezzi, Franco, Jim Jr. Douglas, Michel Fortin, and L. Donatella Marini. "Efficient Rectangular Mixed Finite Elements in Two and Three Space Variables." ESAIM: Mathematical Modelling and Numerical Analysis 21, no. 4 (1987): 581–604. doi:10.1051/m2an/1987210405811.

[9] Arnold, Douglas N., and Ragnar Winther. "Mixed Finite Elements for Elasticity in the Stress-Displacement Formulation." Current Trends in Scientific Computing (2003): 33–42. doi:10.1090/conm/329/05839.

[10] Arnold, Douglas N., Richard S. Falk, and Ragnar Winther. "Finite Element Exterior Calculus, Homological Techniques, and Applications." Acta Numerica 15 (May 2006): 1–155. doi:10.1017/s0962492906210018.

[11] Komatitsch, Dimitri, and Jeroen Tromp. "Spectral-Element Simulations of Global Seismic Wave Propagation-I. Validation." Geophysical Journal International 149, no. 2 (May 2002): 390–412. doi:10.1046/j.1365-246x.2002.01653.x.

[12] Davis, Christopher, June G. Kim, Hae-Soo Oh, and Min Hyung Cho. "Meshfree Particle Methods in the Framework of Boundary Element Methods for the Helmholtz Equation." Journal of Scientific Computing 55, no. 1 (September 25, 2012): 200–230. doi:10.1007/s10915-012-9645-0.

[13] Hall, W. S. "Boundary Element Method." Solid Mechanics and Its Applications (1994): 61–83. doi:10.1007/978-94-011-0784-6_3.

[14] Liu, Lei, Junqi Zhang, Chongmin Song, Carolin Birk, and Wei Gao. "An Automatic Approach for the Acoustic Analysis of Three-Dimensional Bounded and Unbounded Domains by Scaled Boundary Finite Element Method." International Journal of Mechanical Sciences 151 (February 2019): 563–581. doi:10.1016/j.ijmecsci.2018.12.018.

[15] Natarajan, Sundararajan, Ean Tat Ooi, Albert Saputra, and Chongmin Song. "A Scaled Boundary Finite Element Formulation over Arbitrary Faceted Star Convex Polyhedra." Engineering Analysis with Boundary Elements 80 (July 2017): 218–229. doi:10.1016/j.enganabound.2017.03.007.

[16] Liu, Lei, Junqi Zhang, Chongmin Song, Carolin Birk, Albert A. Saputra, and Wei Gao. "Automatic Three-Dimensional Acoustic-Structure Interaction Analysis Using the Scaled Boundary Finite Element Method." Journal of Computational Physics 395 (October 2019): 432–460. doi:10.1016/j.jcp.2019.06.033.

[17] Atluri, S. N., and T. Zhu. "A New Meshless Local Petrov-Galerkin (MLPG) Approach in Computational Mechanics." Computational Mechanics 22, no. 2 (August 24, 1998): 117–127. doi:10.1007/s004660050346.

[18] Yumin, Cheng, and Peng Miaojuan. "Boundary Element-Free Method for Elastodynamics." Science in China Series G: Physics, Mechanics and Astronomy 48, no. 2 (March 2005): 641–657. doi:10.1007/bf02687411.

[19] LIU, G.R., and Y.T. GU. "A Local Radial Point Interpolation Method (Lrpim) For Free Vibration Analyses Of 2-D Solids." Journal of Sound and Vibration 246, no. 1 (September 2001): 29–46. doi:10.1006/jsvi.2000.3626..

[20] Zhu, T., J.-D. Zhang, and S. N. Atluri. "A Local Boundary Integral Equation (LBIE) Method in Computational Mechanics, and a Meshless Discretization Approach." Computational Mechanics 21, no. 3 (April 23, 1998): 223–235. doi:10.1007/s004660050297.

[21] Babuška, Ivo, Fabio Nobile, and Raúl Tempone. "A Stochastic Collocation Method for Elliptic Partial Differential Equations with Random Input Data." SIAM Journal on Numerical Analysis 45, no. 3 (January 2007): 1005–1034. doi:10.1137/050645142.

[22] Roberts, J.E., and J.-M. Thomas. "Mixed and Hybrid Methods." Handbook of Numerical Analysis (1991): 523–639. doi:10.1016/s1570-8659(05)80041-9..

[23] Chen, Linchong, and Xiaolin Li. "Boundary Element-Free Methods for Exterior Acoustic Problems with Arbitrary and High Wavenumbers." Applied Mathematical Modelling 72 (August 2019): 85–103. doi:10.1016/j.apm.2019.03.017.

[24] Chen, L., X. Liu, and X. Li, The boundary element-free method for 2D interior and exterior Helmholtz problems. Computers & Mathematics with Applications, 2019. 77(3): p. 846-864. doi: j.camwa.2018.10.022.

[25] Bu, Weiping, Yifa Tang, Yingchuan Wu, and Jiye Yang. "Finite Difference/finite Element Method for Two-Dimensional Space and Time Fractional Bloch–Torrey Equations." Journal of Computational Physics 293 (July 2015): 264–279. doi:10.1016/j.jcp.2014.06.031.

[26] Khodakarami, M.I. and H.K. Hedayati, DSBFEM AS A MACRO ELEMENT FOR FE ANALYSIS, in the 12th word congress on computional mechanics. 2016: Korea, Seoul.

[27] Khodakarami, M.I., N. Khaji, and M.T. Ahmadi. "Modeling Transient Elastodynamic Problems Using a Novel Semi-Analytical Method Yielding Decoupled Partial Differential Equations." Computer Methods in Applied Mechanics and Engineering 213–216 (March 2012): 183–195. doi:10.1016/j.cma.2011.11.016..

[28] Khodakarami, M.I., and N. Khaji. "Analysis of Elastostatic Problems Using a Semi-Analytical Method with Diagonal Coefficient Matrices." Engineering Analysis with Boundary Elements 35, no. 12 (December 2011): 1288–1296. doi:10.1016/j.enganabound.2011.06.003..

[29] Khodakarami, M.I., and N. Khaji. "Analysis of Elastostatic Problems Using a Semi-Analytical Method with Diagonal Coefficient Matrices." Engineering Analysis with Boundary Elements 35, no. 12 (December 2011): 1288–1296. doi:10.1016/j.enganabound.2011.06.003..

[30] Khaji, N., and M.I. Khodakarami. "A New Semi-Analytical Method with Diagonal Coefficient Matrices for Potential Problems." Engineering Analysis with Boundary Elements 35, no. 6 (June 2011): 845–854. doi:10.1016/j.enganabound.2011.01.011..

[31] Chandrupatla, Tirupathi R., Ashok D. Belegundu, T. Ramesh, and Chaitali Ray. Introduction to finite elements in engineering. Vol. 10. Upper Saddle River, NJ: Prentice Hall, 2002..

[32] Miers, L.S., and J.C.F. Telles. "Meshless Boundary Integral Equations with Equilibrium Satisfaction." Engineering Analysis with Boundary Elements 34, no. 3 (March 2010): 259–263. doi:10.1016/j.enganabound.2009.09.008.